



Research Article

Response of Partly Recrystallized Microstructure to the Rapid Heat Treatment in TC18 Alloy

Fucheng Qiu,¹ Orest Ivasishin,^{1,2,3} Shucheng Dong ,^{1,2} Tuo Cheng ,¹
Dmytro Savvakin,^{1,2,3} and Xinlin Li⁴

¹College of Materials Science and Engineering, Jilin University, Changchun 130025, China

²International Center of Future Science, Jilin University, Changchun 130025, China

³G.V. Kurdyumov Institute for Metal Physics, Kyiv, Ukraine

⁴Key Laboratory of Superlight Materials and Surface Technology, Ministry of Education, Harbin Engineering University, Harbin 150001, China

Correspondence should be addressed to Tuo Cheng; tuocheng@jlu.edu.cn

Received 26 November 2021; Revised 26 January 2022; Accepted 16 February 2022; Published 14 March 2022

Academic Editor: Akbar Heidarzadeh

Copyright © 2022 Fucheng Qiu et al. This is an open access article distributed under the Creative Commons Attribution License, which permits unrestricted use, distribution, and reproduction in any medium, provided the original work is properly cited.

The response of TC18 (Ti-5Al-5Mo-5V-1Cr-1Fe) alloy bar to the rapid heat treatment ($20\text{ K}\cdot\text{s}^{-1}$) in the 850 to 950°C temperature range followed by ageing at 500°C for 8 hours was studied in this paper. Starting material was only partly recrystallized; share of nonrecrystallized part was not uniform along the bar and consisted 10 to 50% of the cross section. Although both parts, recrystallized and nonrecrystallized, had $\alpha+\beta$ phase composition, the morphology of α phase in them was different. Due to that and, presumably, to different defect density, the two parts behaved differently upon rapid heating and ageing keeping the properties fluctuated depending on the fraction of the nonrecrystallized part in the particular specimen since nonrecrystallized material remained harder and stronger and therefore more inclined for microcracks to nucleate and grow. Such fluctuation masked a possible temperature dependence of the properties. It resulted in a strength level of around 1700 MPa which is well above the typical strength of this alloy achieved with conventional thermal hardening. Thus, rapid heat treatment can be successfully used to process an extremely high strength condition in titanium alloys to increase their competitiveness in many attractive applications.

1. Introduction

Titanium alloys become more and more important as a structural material due to their high strength-to-weight ratio, high fatigue strength, and corrosion resistance [1–5]. These properties are attributed to the chemistry and microstructural features (such as grain size, morphology, and substructure) of the phase constituents, which all can be significantly improved by the heat treatment process [6, 7]. The highest strength of titanium alloys is achieved with heat treatment designated as STA (solution treatment followed by ageing). One of the most advanced options of the STA is rapid heat treatment (RHT) in which rapid heating to the temperatures close to the β transus is used instead of furnace solution treatment. The RHT has proved to be an effective

way to optimize the mechanical properties of titanium alloys. The most important feature of the RHT is that high heating rates affect the mechanism and kinetics of $\alpha+\beta$ phase transformation, thus resulting in a formation of modified microstructures in comparison to conventional heat treatment [8, 9]. Microstructural effects associated with RHT include microstructural refinement on a grain size scale as well as a formation of finer microstructural components in the grain interiors due to microchemical inhomogeneity and substructure of the high-temperature β phase. An increase of the β transus temperature above its equilibrium value was found to be proportional to the logarithm of the heating rate.

However, the result of RHT is affected by many factors. It was established in [8] that, for the same heating rate, the

influence of heating rate depends on the type of titanium alloys and is more pronounced for the alloys with high content of the β stabilizers; for the same alloy, it depends on the morphology (shape and size) of the α phase grains. The last finding is a very important for practical application of the RHT since it clearly indicates that RHT parameters should be carefully correlated with the starting microstructure of the alloys. Moreover, it puts a strong requirement to the starting microstructure regarding its uniformity; otherwise, a nonuniformity of the structure and properties through the treated part will appear. This was the reason why a majority of research efforts demonstrating positive effects of the RHT were done on the alloys with starting equiaxed microstructure which is the most suitable for such treatment from the viewpoint of its uniformity [10–12].

RHT of the alloys with metastable starting microstructure formed by thermomechanical processing is also possible but it is used mostly for the metastable beta alloys in which starting microstructure is formed by highly intensive cold deformation. RHT of the deformed materials is considered as an advantageous processing route since it gives a possibility to get finer and more uniform grain sizes upon recrystallization due to a higher density of nuclei while displacing upward the recrystallization temperature [13–15]. Another advantage of such treatment can be a possibility to preserve some amount of deformation defects in the high temperature β phase substructure what has a marked influence on its microstructure and properties.

A requirement of uniformity of starting microstructure is most difficult to perform in the alloys which thermomechanical processing starts above but finished below the β transus. As a rule, the microstructure of such alloys is presented as a mixture of recrystallized (*R*) and non-recrystallized (*NR*) parts, each part having its own microstructural parameters. Taking into account the above described features of the RHT, the response of alloys with such starting microstructure is hard to predict since phase transformations in the *R* and *NR* parts will expectedly proceed differently. Moreover, further recrystallization is possible in the *NR* part upon RHT. To our knowledge, this paper will be a first attempt to apply the RHT to the partly recrystallized titanium alloy.

The material under investigation was the TC18 alloy. Its nominal composition is Ti-5Al-5Mo-5V-1Cr-1Fe (Ti55511). As a high strength titanium alloy, it is designed for structural applications, such as landing gear components. By its composition, it is closed to the Russian VT22 and TIMET 555(Ti-5Al-5Mo-5V-3Cr-0.5Fe) alloys. Compared to Ti-6Al-4V, another widely used in the aerospace industry alloy, Ti55511 is better structural material because of its higher strength-to-weight ratio which can provide 15–20% weight reduction [16]. Ti55511 is also a good candidate to replace Ti1023 alloy, due to its higher strength, wider processing window and better hardenability [17]. Moreover, the Ti55511 has shown an ability to serve at temperatures about 350°C [18].

Mechanical properties of Ti55511 and similar alloys are strongly depending on the β grain size, morphology of α precipitates, and recrystallization degree. This means that

their microstructure and properties can be significantly modified by heat treatments. No research efforts have been done so far on the RHT of TC18. However, this was done earlier for the similar VT22 alloy. In [19], VT22 was undergone to the RHT and it was shown that its strength increased independently of cooling method used (water quenching or air cooling). RHT was also applied to the cold deformed VT22 [20–22]. Formation of fine recrystallized β grains and strictly controlled precipitation behavior upon ageing resulted in a very high ultimate tensile strength of 1755 MPa [20]. Specifically, the effect of heating rate to ageing temperature on ageing behavior of VT22 was also studied which allowed the provision of the most optimal mechanism of β phase decomposition.

All above cited studies on the RHT of the VT22 alloy were performed on the material which starting microstructure could be characterized as uniform, either annealed [21] or deformed [20, 22]. The objective of this paper was to apply the RHT to the bar material processed in such a way that its microstructure was partially recrystallized. The study was focused on the influence of recrystallization degree on the alloy response to the RHT since we found that such microstructure type is rather typical, at least for this alloy bar and plate products.

2. Material and Methods

The TC18 alloy (bar of 12 mm in diameter) was bought from commercial company; its chemical composition is shown in Table 1. Bar pieces 70 mm long were rapidly heated to 850°C, 875°C, 900°C, 910°C, 925°C, 940°C, and 950°C in the intermediate frequency inductor with heating rate of 20°C/s, followed by immediate water quenching. After quenching, all specimens were directly aged at 500°C for 8 hours. The pick temperature of the rapid heating was measured by infrared temperature probe (IRTD-1500LS) installed at the distance of 20 mm from the sample surface.

Microstructure of the starting and heat treated samples was revealed by Kroll reagent (2%HF+5%HNO₃+93%H₂O) or, in case of aged samples, by its tenfold diluted option. The microstructure pictures were taken from both longitudinal and transverse sections. To establish any interrelation between the microstructure and mechanical properties, transverse sections of the tensile specimens were done close to the fracture surfaces. The microstructure characterization of as-received TC18 alloy was performed by optical microscopy (OM) and SEM at the operating voltage of 20 kV. The microstructure characterization of samples after rapid heat treatment was performed by thermal field emission SEM. Phase composition before and after heat treatments was controlled by XRD technique using Rietveld method for the calculation of the amounts of phase constituents.

Special attention was paid to estimation of recrystallized (*R*) and nonrecrystallized (*NR*) parts in the samples before and after the heat treatment. Respective calculations were performed with the help of Image-pro 6.0 software at the central areas of the transverse sections. Beta grain sizes were measured in the recrystallized parts.

TABLE 1: The chemical composition of TC 18 alloy.

Element	Al	Mo	V	Cr	Fe	O	N	H	Ti
Wt%	5.03	5.02	5.03	1.02	1.00	0.095	0.01	0.0061	Bal.

Vickers hardness was measured under load of 1000g and dwell time of 10s. Tensile tests were performed using cylindrical specimens with a gauge diameter of 5 mm and gauge length of 25 mm. At least three specimens of each condition were tested.

3. Results

3.1. As-Received State. Figure 1 shows the typical microstructure of the as-received alloy. It is complex and not uniform. It consists of two different parts, recrystallized (*R*) and nonrecrystallized (NR), with a well resolved boundary between them (Figures 1(a)–1(c)). NR and *R* parts continuously distribute over a fairly long range in longitudinal direction of the bar (Figures 1(d) and 1(e)). Such a structure was formed by high temperature deformation that promoted a formation of elongated in the rolling direction grains; some part of them dynamically recrystallized. The average size of recrystallized grains was about 20 μm although the grains located near the *R*/NR boundary were smaller. It was possible to distinguish the NR and *R* parts not only in the longitudinal but also in the transverse sections as well (Figures 1(a) to 1(c)). Comparing microstructures in longitudinal and transverse sections allows us to conclude that NR grains have a very high aspect ratio indicating a significant reduction upon deformation that, however, did not result in a full recrystallization. Because of nonuniform distribution of the NR grains and their specific shape, relative portions of the *R* and NR parts vary significantly along the bar.

XRD analysis of the as-received material showed a typical $\alpha + \beta$ phase composition. The total mass fraction of α phase was determined by Rietveld refinement from XRD data whose comparison between the experimental and calculated one is given in Figure 2. The total fraction of α phase was calculated as 51%. It was interesting that Rietveld analysis showed that β phase was presented by two modifications having different lattice parameters 3.229 and 3.255 \AA , presumably belonging to different parts, *R* and NR, of the material.

Quite expectedly, the morphology of α phase was too much extent different in the *R* and NR parts. In *R* part, the recrystallized grains are decorated by a layer of α phase, mostly of continuous type while an intragrain α forms groups (colonies) of individual lamellas whose thickness and length vary from 0.11 to 0.26 and from 0.87 to 3.25 micrometers correspondingly (Figures 3(a) and 3(b)). In general, thickness of the grain boundary α phase is bigger than that of the individual lamellas. The areas close to the grain boundaries are generally free from α phase; sometimes α phase of the nearly spheroidized shape is observed. More complicated is a diversity of α phase morphology formed in the NR parts. A plenty of long and straight α phase layers were formed on various type boundaries or subboundaries

and slip bands. Sometimes these layers are fragmented because of a preferable α precipitation on a specific crystallographic plane. It is well seen on the microstructures related to the transverse sections that plenty of α lamellas grew perpendicular to these long straight α layers or, more exactly, to the boundaries decorated by them (Figure 3(d)). There were also rather large areas in the NR parts without grain boundaries inside in which α phase of such morphology was not observed (Figure 3(c)). Alpha phase in between these specific long straight layers was of nearly the same morphology as described above for the *R* part.

Tensile properties of the as-received material were rather typical for this type alloys, namely, UTS of 1054 MPa at 22% elongation. These numbers, however, show that this condition has a big potential for the thermal hardening by heat treatment. Figures 4(a)–4(c) showed the fracture features in as-received specimens. The fracture surface of as-received materials can be divided into two regions. As shown in Figure 4(b), large and deep dimples can be seen in the centre region. The dimples in the rim region are shallow and some tear ridges are shown clearly in the fracture surface. Parabolic dimples are observed in these two regions. The parabolic dimples elongated along the tear ridges in the rim region confirm the ductile of fracture [23].

3.2. Solution Treated (RHT) Condition. Thermoresistometric study showed that β transus temperature increased to 910°C at heating rate of 20°C/s (Figure 5). Compared to equilibrium β transus temperature (860°C), the increase was around 50°C. Therefore, samples heated to temperatures below this temperature were still in the two-phase $\alpha + \beta$ condition while samples heated to 925°C and 940°C reached the single phase β field. XRD analysis of the respective samples water quenched from these temperatures confirmed that, as shown in Figures 6(a) and 6(b), taking samples heated to 860°C and 925°C as examples of these two typical groups treated below and above the β transus. The α phase content at 860°C was 15%, while XRD analysis fixed single phase β condition after heating to 925°C. Microstructural observations (some of them are presented in Figures 7 and 8) gave a clear evidence that fine α particles were first to dissolve at subtransus temperatures; the remnants of α phase were certainly related to the grain boundary α layers and, sometimes, to the relatively thick α plates in the interiors of the *R* and NR parts. Because of a pronounced structure nonuniformity and a very fine α lamella sizing, it was not easy to make a conclusion on a development of recrystallization upon rapid heating changing a relative share of the *R* part and to distinguish in what part, *R* or NR, kinetics of α dissolution was faster. However, there were some indications that this process developed more effectively in the recrystallized β grains (compare Figures 7(a) and 7(b)). The grain growth became evident in the β phase field but the grain size remained very not uniform (Figure 7(e)).

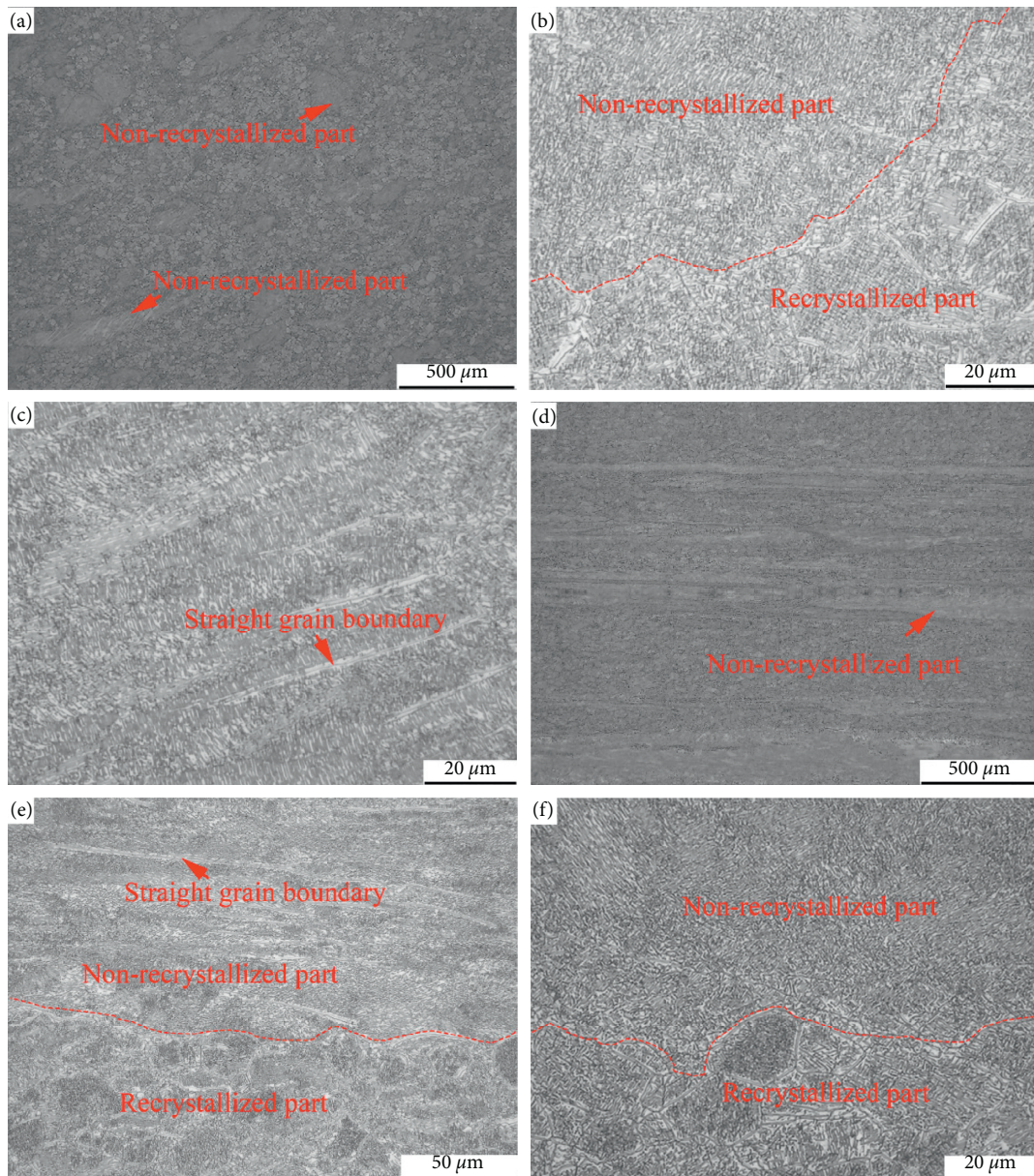


FIGURE 1: Micrographs of as-received materials: (a)-(c) at transverse sections; (d)-(f) at longitudinal sections.

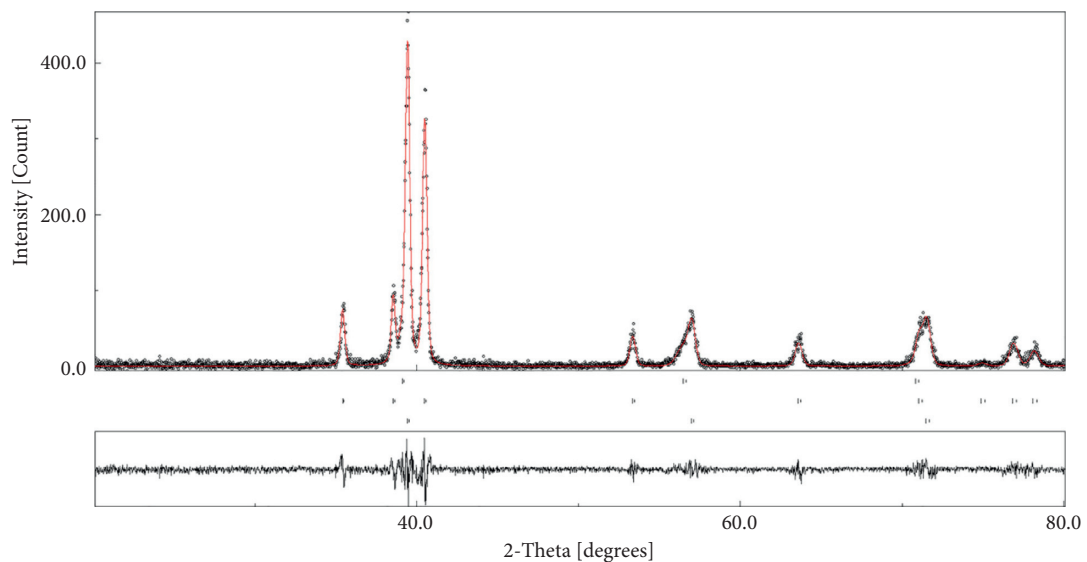


FIGURE 2: XRD pattern of the as-received material.

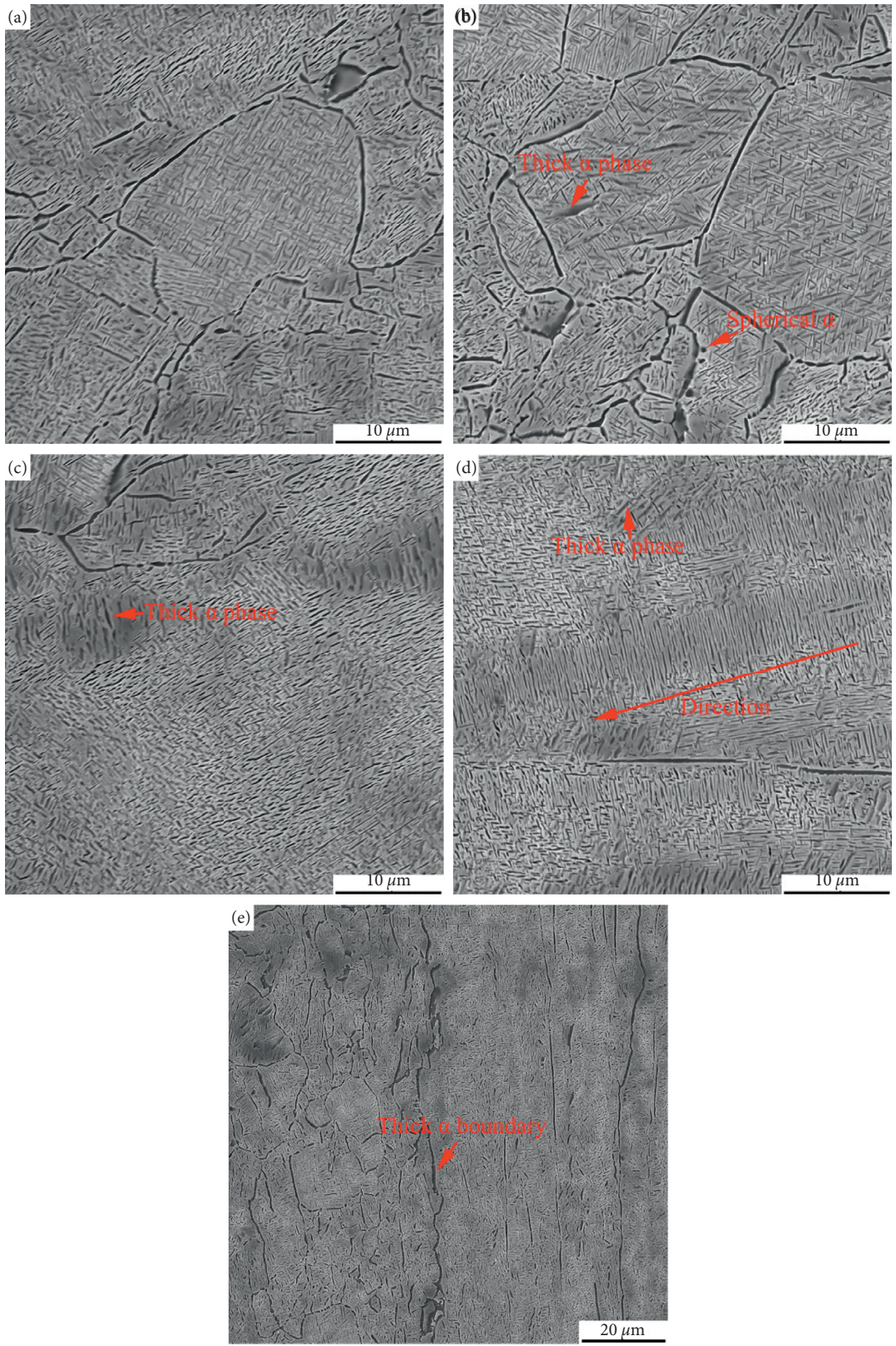


FIGURE 3: SEM of as-received materials: (a) and (b) in recrystallized parts; (c) and (d) in nonrecrystallized parts; (e) the SEM at longitudinal section.

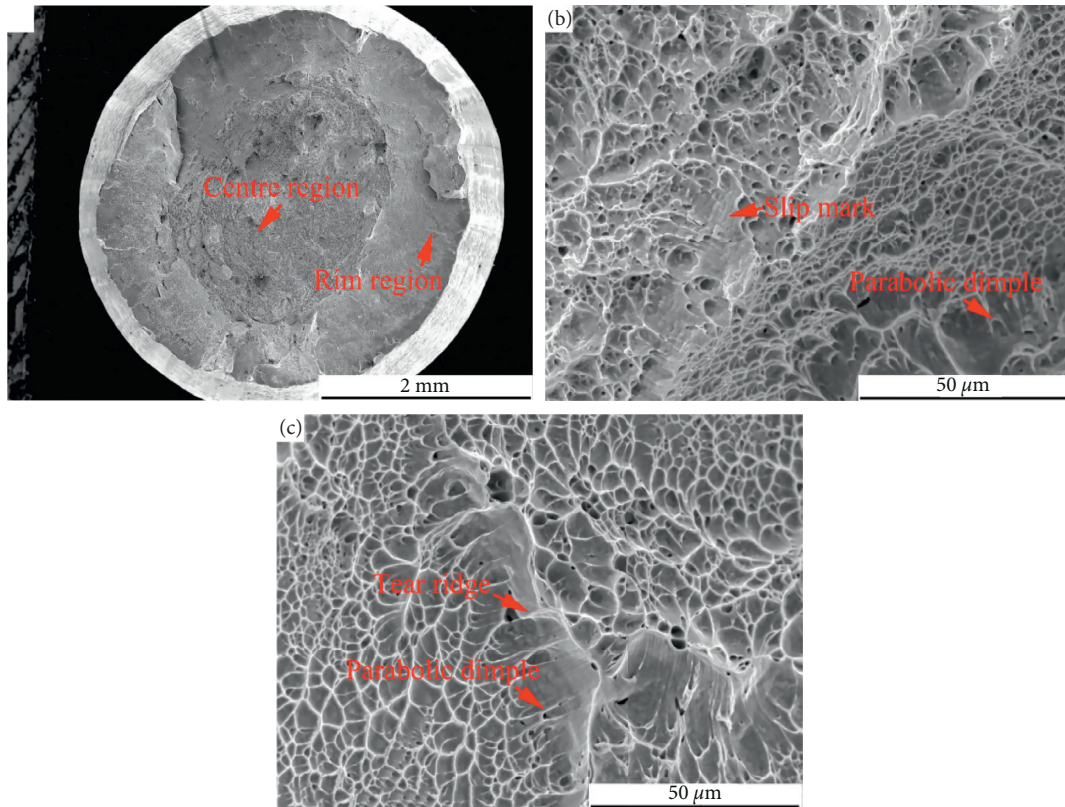


FIGURE 4: (a) Fracture surface of as-received materials; (b) and (c) the magnification of centre and rim regions in (a).

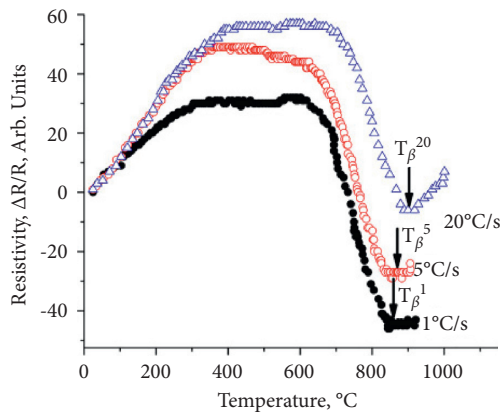


FIGURE 5: Relationship between the RHT temperature and resistivity at different heating rates.

3.3. Solution Treated (RHT) and Aged Condition

3.3.1. Microstructure. Ageing at 500°C for 8 hours resulted in a formation of fine α precipitates in a metastable β phase fixed by water quenching. The α phase exhibited different characteristics in the R and NR parts. And the difference of characteristics was more pronounced if the temperature of rapid heating was below the β transus. As is seen in Figure 8(a), after heating to 860°C, the α showed diverse morphology in the NR part; some remnants of the starting α lamellas coexisted with much finer precipitates. In the temperatures above the beta transus (925 C and 940 C,

Figures 8(b) and 8(c)), all α precipitates were newly formed but still not uniformly distributed and sized. A very interesting α morphology consisting of a crystallographically equivalent fine precipitates was formed along the former grain boundaries decorated with long α layers (Figure 3). Such layers transformed to β at the last stages of the rapid heating and therefore had the lowest content of the β stabilizers (corresponding difference in the β composition is well seen on the SEM picture, Figure 8(c)). Compared to the NR part, the morphology of α precipitates was more uniform in recrystallized β grains and only slightly changed with temperature crossing the β transus (Figures 9(a) and 9(b)). The precipitates formed a typical for this kind of phase transformation crystallography of the precipitates.

3.3.2. Mechanical Properties. Tensile properties of the alloy in the solution treated and aged condition are presented in Figures 10 and 11, as function of the RHT temperature. It is well seen that the strength (presented by UTS value) greatly increased while ductility (presented as the elongation value) decreased significantly, compared to the starting condition. This result was fully in line with the microstructural observation and XRD results indication on the transformation of a relatively coarse α phase to much finer α precipitates. However, the strength and ductility values did not show a clear dependence on the RHT temperature within the temperature interval used. Moreover, the properties received after the treatment at the same temperature varied substantially. As an example, the UTS value of the samples

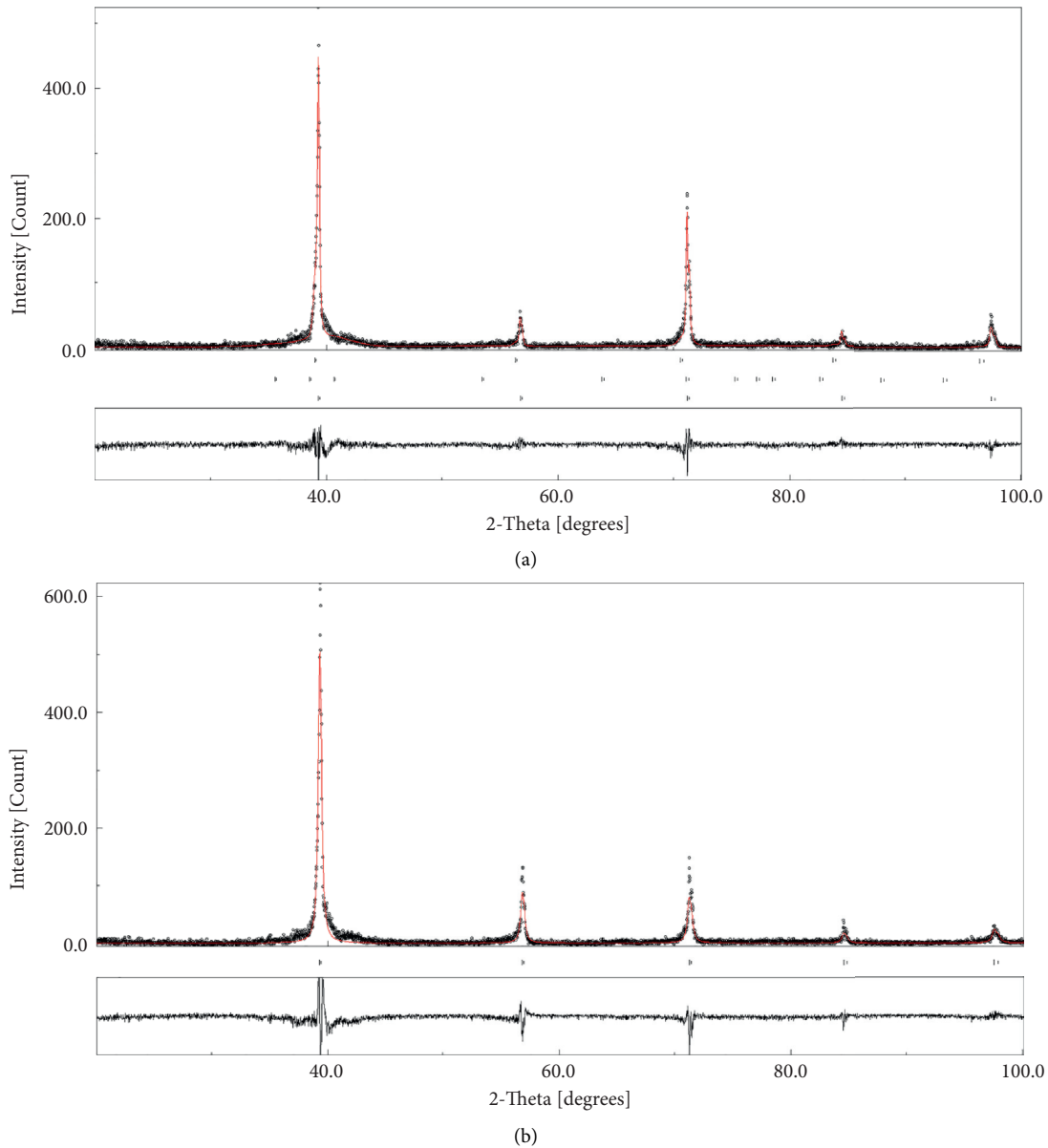


FIGURE 6: The XRD pattern of (a) samples rapidly heated to 860°C and (b) samples rapidly heated to 925°C followed by quenching.

treated at 875°C varied from 1700 to 1770 MPa; corresponding elongation values were in the 3.28% to 1.36% range. It was found from microstructural observations that a variation of these properties was in line with the NR fraction in the particular sample: the higher the NR fraction, the higher strength and lower ductility the alloy received by the treatment at this particular temperature (Figure 12). Since it was impossible to measure the strength and ductility of the NR and *R* parts separately, their hardness was measured for all treated samples after their mechanical testing (Figure 13). It was found that the average hardness of the NR parts was higher than that in *R* parts for most of the RHT temperatures and became close to it only when the RHT temperature was 950°C. The highest hardness was found to be in the alloy treated at 875°C, for both NR and *R* parts, slightly decreasing then for the higher RHT temperatures, what corresponded

to the similar trend in a change of tensile strength. A variation in NR/*R* relation as a function of the RHT temperature (Figure 14) was certainly accidental, not really depending on the temperature but rather defined by this relation in the particular starting samples. However, just this relation was responsible for the biggest part of the properties variation. Another part of the properties change that hardly can be estimated may be speculated as a result of microstructural reaction to the temperature, such as a dependence of α precipitation mechanism and kinetics on the composition gradients and defect structure of the β phase formed upon rapid heating [24–27]. As an example, the highest strength achieved at 875°C RHT can be attributed to the faster α precipitation on the defects remaining from the starting condition. With the RHT temperature approaching or especially being above the β transus, this advantage was

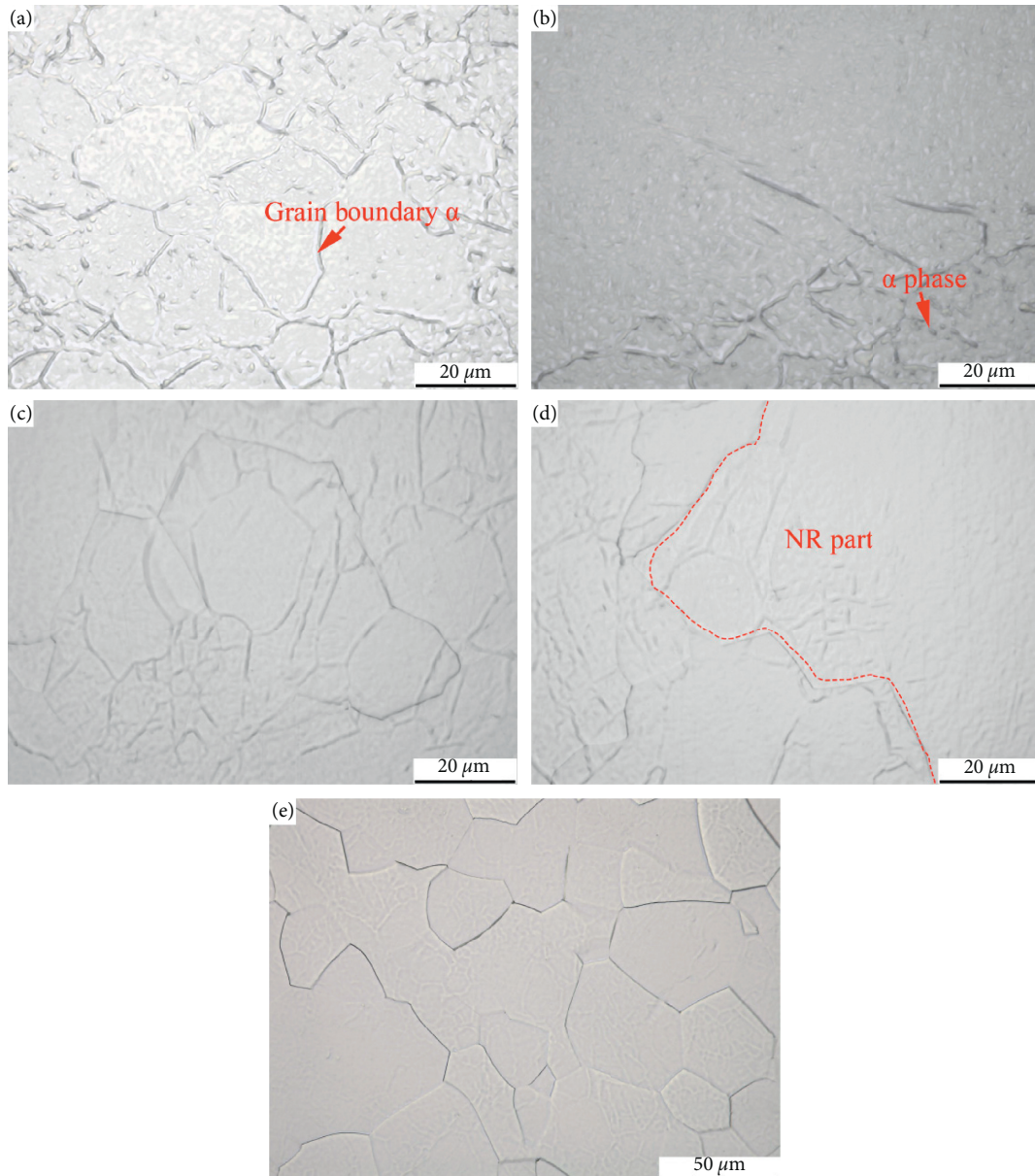


FIGURE 7: (a) R part and (b) NR part of samples rapidly heated to 860°C followed by quenching; (c) R part and (d) NR part of samples rapidly heated to 925°C followed by quenching; (e) the microstructure of samples rapidly heated to 940°C followed by quenching.

certainly lost. Another maximum strength achieved at RHT temperature of 925°C could have another nature related to full transformation of the starting α phase into the β and, therefore, the highest possible strengthening. However, such treatment causes a further degradation of the ductility, presumably because of the grain growth in the β phase field.

As shown in Figure 15(a), the fracture surfaces of specimens after RHT and ageing could be divided into two regions, center and rim ones. The surfaces were relatively flat in the rim regions; shallow dimples, smooth facets, tear ridges, and, sometimes, few cleavage facets were their main characteristics (Figures 15(b) and 15(c)). Fracture surfaces of the rim regions showed no apparent difference for specimens with different NR share treated at the same temperature. However, a relative fraction of the particular features

changed when the RHT temperature increased, as can be seen from the comparison of fracture surfaces of the samples treated at 875°C and 950°C. An increase of smooth facet areas and cleavage facets was observed in the specimens treated at higher temperature.

Fracture surfaces in center region corresponded to a typical mixed mode. Dimples and cleavage facets could be observed in all specimens. As shown in Figures 16(a) to 16(c), an increase of NR share resulted in an increase of the large facets fraction. From the microstructural observations of the close to the fracture surface areas (not presented here), it could be suggested that the large facets in Figures 16(b) and 16(c) were localized in the NR parts. Microcracks were observed on the fracture surfaces; a very important observation was that microcracks located near the large facets

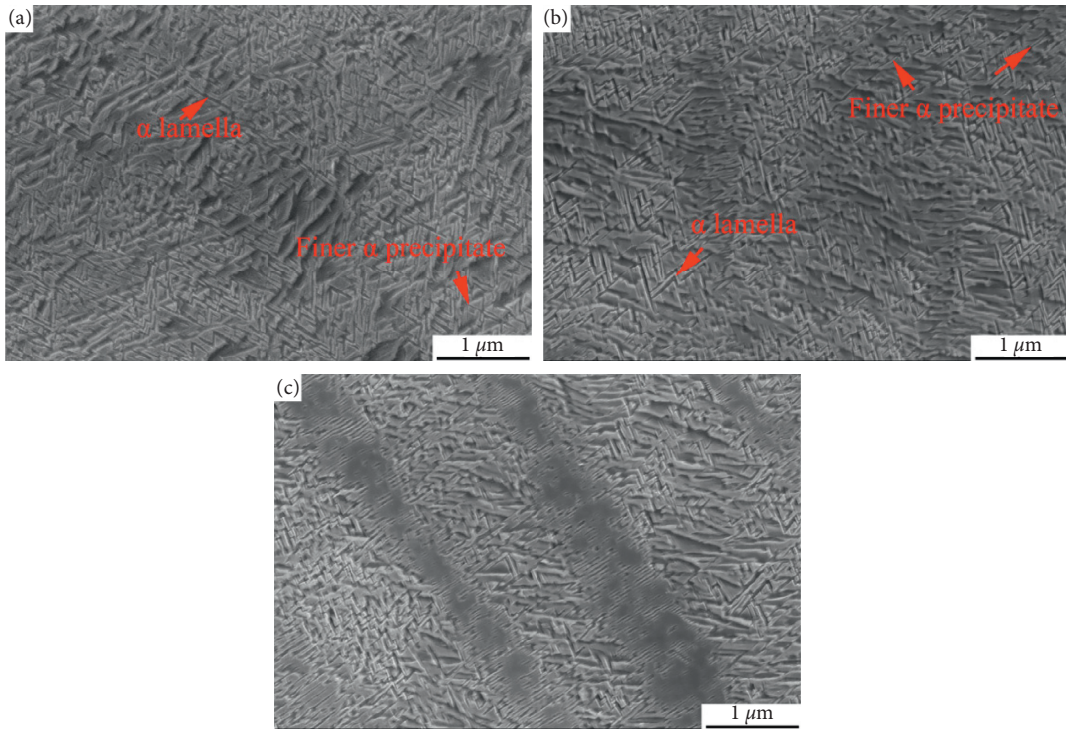


FIGURE 8: Thermal field emission SEM in NR part of (a) specimens rapidly heated to 860°C, (b) specimens rapidly heated to 925°C, and (c) specimens rapidly heated to 940°C followed by ageing.

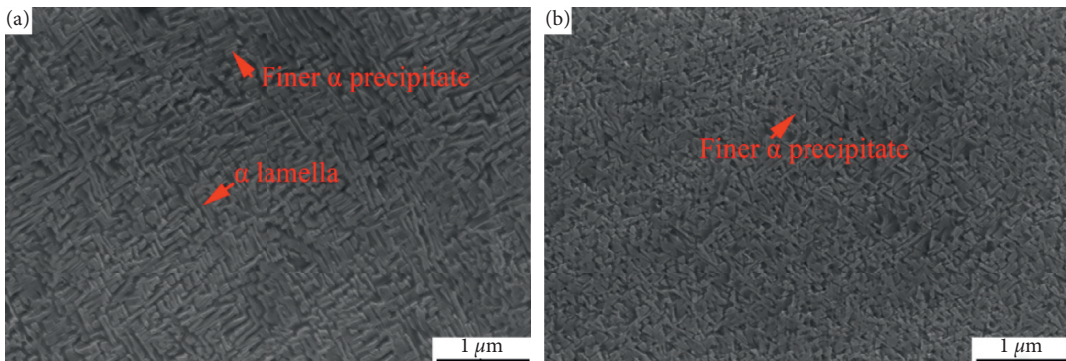


FIGURE 9: Thermal field emission SEM in recrystallized β grains of (a) specimens rapidly heated to 860°C and (b) specimens rapidly heated to 925°C followed by ageing.

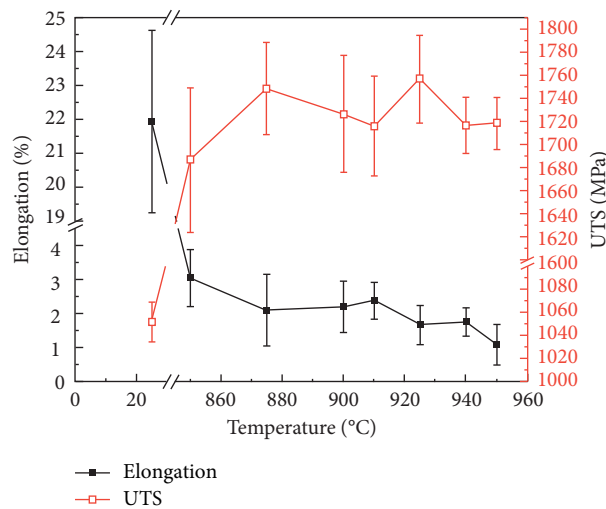


FIGURE 10: The tensile properties of specimens that underwent rapid heat treatment and ageing.

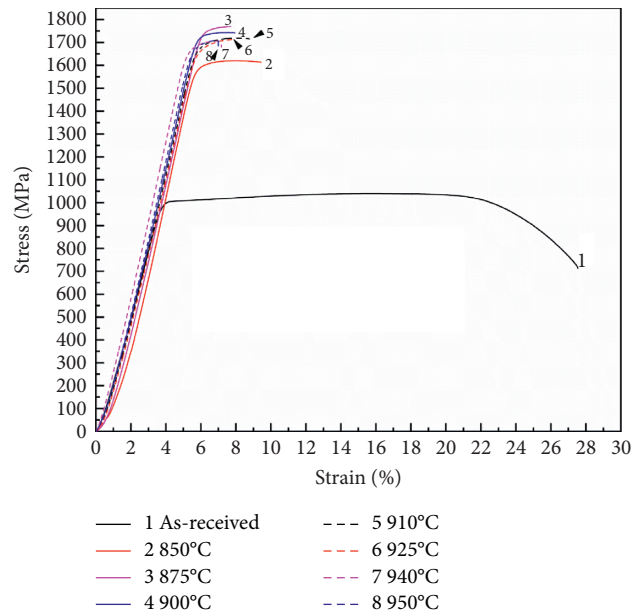


FIGURE 11: The stress-strain curve of as-received specimen and samples after rapid heat treatment followed by ageing.

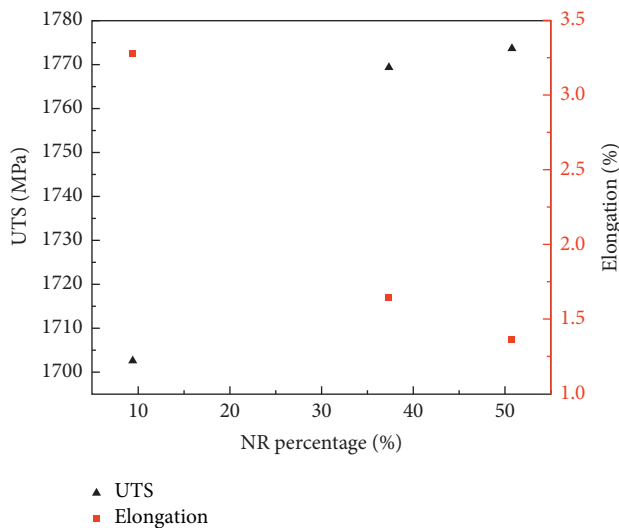


FIGURE 12: The relationship between tensile properties and NR percentage of specimens rapidly heated to 875°C followed by ageing.

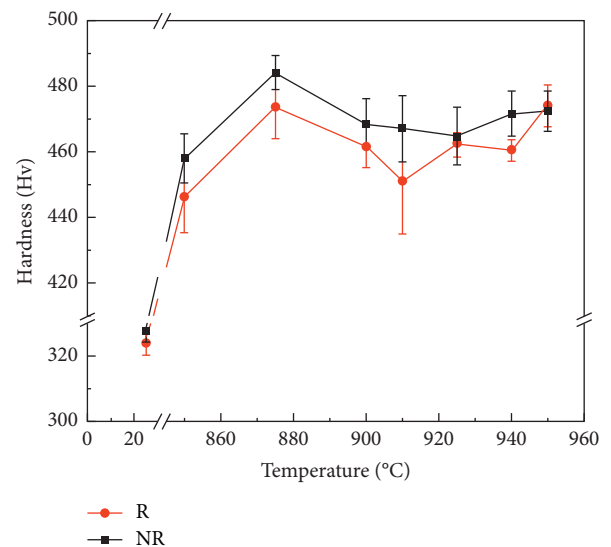


FIGURE 13: Vickers hardness in R and NR parts of specimens that underwent RHT and ageing.

were rather large and long indicating that the microcracks were easier to generate and grow in the NR parts. Therefore, the number of microcracks in the specimen with high NR share was apparently larger. Besides, cleavage steps were observed in the specimens with high NR share, as shown in Figures 16(b) and 16(c). Altogether, this could be the reason of lower ductility of specimens with high NR share, as is shown in Figure 12.

Increase of cleavage facets presumably being a reason for a lower ductility was also observed in the specimens treated above the β transus (Figure 16(d)); in this case it was stimulated by the β grain growth.

4. Discussion

A goal of any thermal hardening of titanium alloys consists in full or at least partial transformation of starting, relatively coarse $\alpha+\beta$ microstructure into the much finer alternative. Considering the higher amount of the starting microstructure that underwent such transformation, the higher strengthening effect is achieved [28]. The results of this paper confirm this statement: tensile strength of the starting material increased from around 1000–1100 MPa to the level of around 1700 MPa, very promising for many applications requiring high strength titanium based materials. A first stage of such

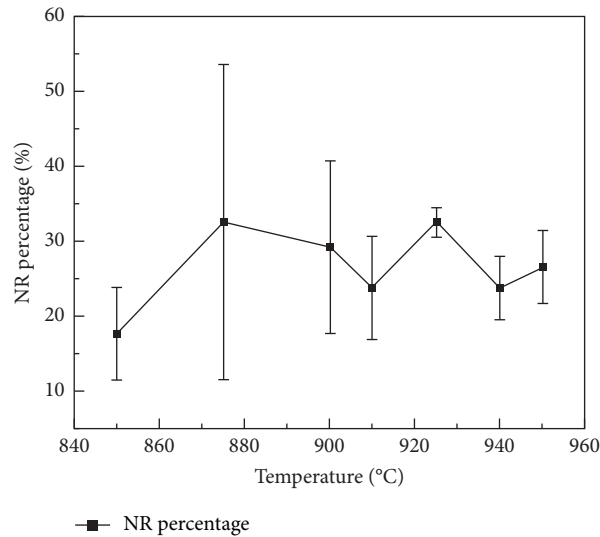


FIGURE 14: The average NR percentage of specimens at different RHT conditions.

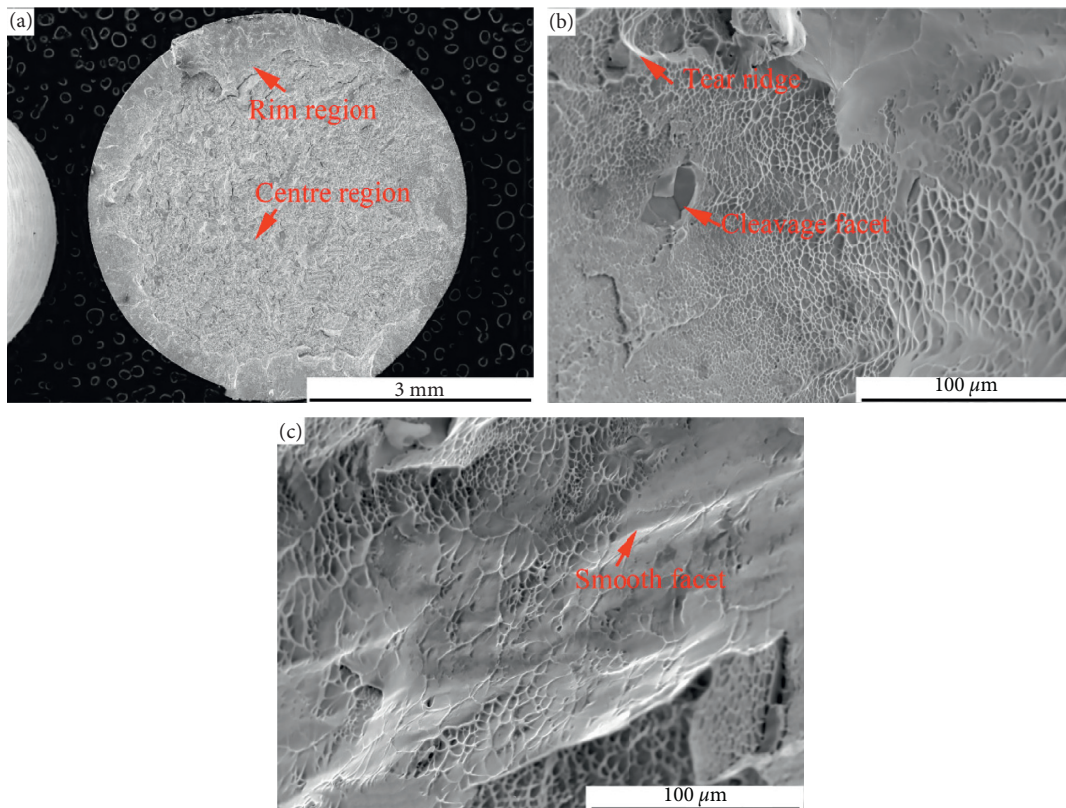


FIGURE 15: (a) Fracture surface of specimens after RHT and ageing; (b) and (c) rim regions of specimens after rapidly heating to 875°C and 950°C followed by ageing.

treatment, sometimes called for simplicity as α phase dissolution, has generally a limit to be performed in the two-phase field only because of a catastrophic grain growth above β transus. The treatment used in this paper whose distinctive feature is rapid heating for an α phase dissolution allowed heating to both two-phase and single β phase temperatures since the growth of β grains was

markedly reduced at temperatures above the β transus. Moreover, at such a treatment, just heating to the temperatures around the β transus is commonly recommended since this provides fuller volume share of the thermally hardened microstructure [8, 29–31].

It should be mentioned that final balance of the strength and ductility is achieved upon ageing. We have

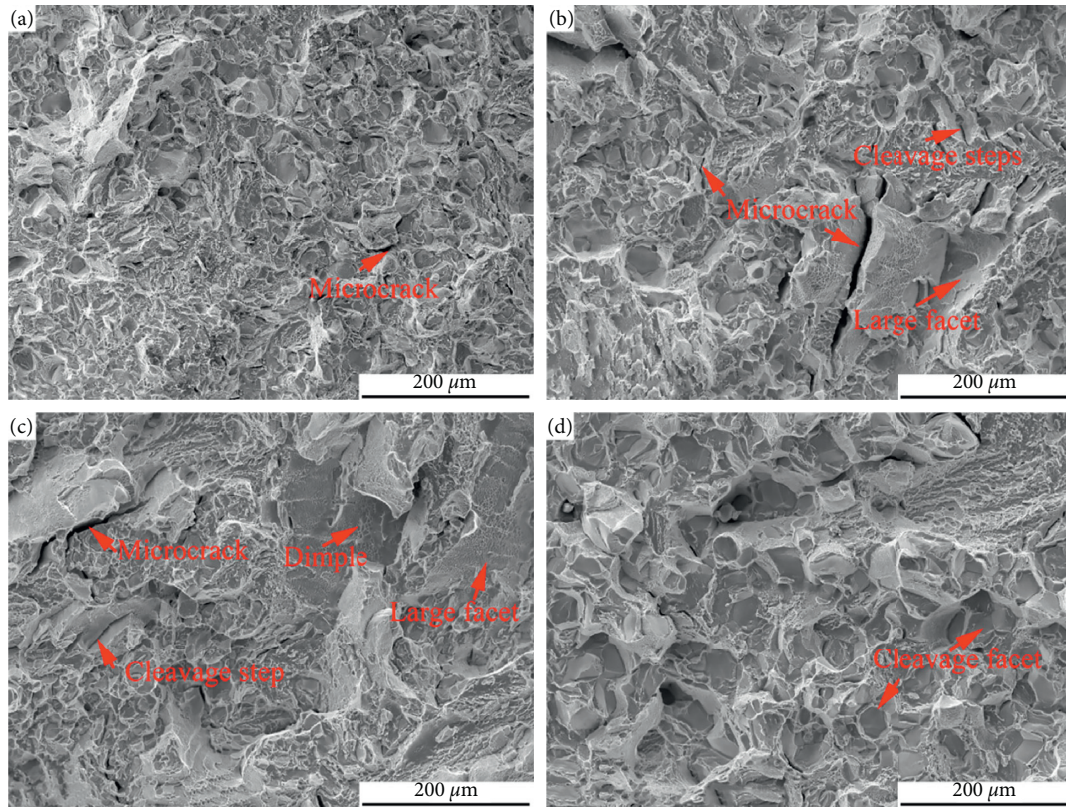


FIGURE 16: The centre regions of specimens with (a) 9.42% NR percentage, (b) 37.36% NR percentage, and (c) 50.75% NR percentage after rapidly heating to 875°C and directly ageing at 500°C for 8 hours; (d) centre region of specimen with 34.62% NR percentage after rapidly heating to 950°C and directly ageing at 500°C for 8 hours.

to recognize that ageing regime used in this paper (500°C, 8 hours, standard for a conventional STA treatment of this alloy [32]) was not properly selected for the case of the RHT. It was found earlier that the alloys treated with using of the rapid heating require modified ageing regimes, i.e., higher ageing temperatures and/or controlled heating rate to the ageing temperature [20, 32, 33]. This requirement came from peculiarities of the metastable β phase formed upon rapid heating, first of all, of its compositional inhomogeneity. Such modification would, of course, lead to some lower strength but its better balance with the ductility. Control experiments showed that, after ageing at 550°C for 6 hours, the elongation increased to 4.8% without a visible in the strength. Work on optimization of ageing is planned for a future research program, having in mind that the current first-order goal was to understand whether the RHT is applicable to the titanium alloys, where starting microstructure was not specially prepared for a better response to such a treatment. The most optimal starting microstructure should be morphologically uniform as much as possible (regarding the shape, close to equiaxed, and the size of α phase). Since preparation of such microstructure needs a strictly controlled thermomechanical processing, it hardly can be the only prerequisite for the practical using of the RHT. Results received in this paper give a background for a statement that a high strength conditions can be successfully obtained in titanium alloys like TC18

even if their starting microstructure does not satisfy the above requirements.

Main microstructural feature of the particular starting microstructure was coexisting of two different parts, R and NR. In general, the NR share was less than 50% but its distribution was not uniform along the bar. It is well understood that, due to different dislocation density in these two parts, they behave differently even in the starting material [34]. The α lamellas were more uniform by size and shape in recrystallized β grains, compared to those in NR parts; hardness in recrystallized grains was expectedly lower. The difference between R and NR parts remained during rapid heating, and even after final ageing, leaving their hardness different until the highest RHT temperature of 950°C (Figure 13).

Since the NR parts were harder, i.e., stronger, they were more difficult to deform [35]; microcracks were easier to generate and grow in the NR parts. Hence, at the same RHT temperature, the specimens with higher NR share showed higher strength and worse ductility, as shown in Figure 12.

RHT followed by ageing changed the deformation mechanism of the alloy under investigation. Only dimples and tear ridges were found in the fracture surface of original material and the elongated parabolic dimples indicated that shear failure was the main failure mechanism [36]. Slip marks in Figure 4(b) also confirmed that slip was the main deformation mechanism in starting material.

In the RHT treated specimens, brittle fracture became the main failure mechanism. Appearance of smooth cleavage facets in center regions and smooth facets in rim regions demonstrated that the ductility of specimens was degrading. Area fraction of cleavage facets increased with increase of RHT temperature indicating growing brittleness. Several reasons were responsible for that. Among them, one can suggest the decrease of α lamellas width in both R and NR parts (Figures 8 and 9) causing higher strains around them and some grain growth at temperatures above the beta transus. Unfortunately, it was impossible to estimate a specific input of the separate processes into the ductility degradation because of a varying NR/R relation in each specimen. However, the ductility would certainly improve with modification of the ageing regime.

5. Conclusion

The rapid heat treatment (RHT) that included heating with a rate of 20°C/s and ageing at 500°C for 8h was applied to TC18 alloy and the following conclusions were drawn:

- (1) As-received condition of the alloy under investigation consisted of recrystallized (R) and non-recrystallized (NR) parts; R/NR relation was not uniform along the length of the bar.
- (2) Behavior of the R and NR parts upon rapid heating was different. Strong dependence of the final microstructure and properties on the R/NR relation in the particular sample was observed which overshadowed an influence of the temperature.
- (3) NR parts exhibited higher hardness after the RHT; microcracks were easier to generate and grow near the NR regions which predetermined worse ductility in the samples having higher NR fraction.
- (4) High strength in excess of 1700 MPa was achieved with such a treatment due to complex transformation of the starting microstructure although such high strength was not well balanced with the ductility.
- (5) For the better response of the TC18 alloy to the RHT, optimization of the starting microstructure regarding its uniformity would certainly be useful and modification of the ageing regime is necessary for the better strength/ductility balance.

Conflicts of Interest

The authors declare that they have no competing financial interests or personal relationships that could have appeared to influence the work reported in this paper.

Acknowledgments

This work was financially supported by the Open Project of Key Laboratory of Superlight Materials and Surface

Technology of Ministry of Education of Harbin Engineering University (No. HEU10202114).

References

- [1] D. Banerjee and J. C. Williams, "Perspectives on titanium science and Technology," *Acta Materialia*, vol. 61, no. 3, pp. 844–879, 2013.
- [2] R. R. Boyer, "Titanium for aerospace: rationale and applications," *Advanced Performance Materials*, vol. 2, no. 4, pp. 349–368, 1995.
- [3] B. Callegari, J. P. Oliveira, K. Aristizabal et al., "In-situ synchrotron radiation study of the aging response of Ti-6Al-4V alloy with different starting microstructures," *Materials Characterization*, vol. 165, Article ID 110400, 2020.
- [4] J. P. Oliveira, B. Panton, Z. Zeng et al., "Laser joining of NiTi to Ti6Al4V using a Niobium interlayer," *Acta Materialia*, vol. 105, pp. 9–15, 2016.
- [5] B. Callegari, J. P. Oliveira, R. S. Coelho et al., "New insights into the microstructural evolution of Ti-5Al-5Mo-5V-3Cr alloy during hot working," *Materials Characterization*, vol. 162, Article ID 110180, 2020.
- [6] S. L. Nyakana, J. C. Fanning, and R. R. Boyer, "Quick reference guide for β titanium alloys in the 00s," *Journal of Materials Engineering and Performance*, vol. 14, no. 6, pp. 799–811, 2005.
- [7] J. Fan, J. Li, H. Kou, K. Hua, B. Tang, and Y. Zhang, "Microstructure and mechanical property correlation and property optimization of a near β titanium alloy Ti-7333," *Journal of Alloys and Compounds*, vol. 682, pp. 517–524, 2016.
- [8] O. M. Ivasishin and P. E. Markovsky, "Enhancing the mechanical properties of titanium alloys with rapid heat treatment," *Jom*, vol. 48, no. 7, pp. 48–52, 1996.
- [9] V. N. Gridnev, O. M. Ivasishin, and P. E. Markovskii, "Influence of heating rate on the temperature of the (β ?) \rightarrow (α ?) transformation of titanium alloys," *Metal Science and Heat Treatment*, vol. 27, no. 1, pp. 43–48, 1985.
- [10] S. Rhaipu, "The effect of rapid heat treatment on the high-temperature tensile behavior of superplastic Ti-6Al-4V," *Metallurgical and Materials Transactions A*, vol. 33, no. 1, pp. 83–92, 2002.
- [11] D. Ao, X. Chu, Y. Yang, S. Lin, and J. Gao, "Effect of electropulsing treatment on microstructure and mechanical behavior of Ti-6Al-4V alloy sheet under argon gas protection," *Vacuum*, vol. 148, pp. 230–238, 2018.
- [12] Y. Zhao, Y. Shi, X. Yang, and X. Xu, "Rapid strengthening without loss of ductility via electropulsing treatment in Ti-6Al-4V alloy," *Journal of Materials Engineering and Performance*, vol. 27, no. 7, pp. 3636–3642, 2018.
- [13] Y. B. Wang, Y. F. Zheng, and Y. Liu, "Effect of short-time direct current heating on phase transformation and superelasticity of Ti-50.8at.%Ni alloy," *Journal of Alloys and Compounds*, vol. 477, no. 1-2, pp. 764–767, 2009.
- [14] O. M. Ivasishin and R. V. Teliovich, "Potential of rapid heat treatment of titanium alloys and steels," *Materials Science and Engineering: A*, vol. 263, no. 2, pp. 142–154, 1999.
- [15] Y. Y. Fu, S. X. Hui, W. J. Ye, and X. J. Mi, "Influence of heat treatment on microstructure and tensile property of Ti-5Al-5Mo-5V-3Cr-1Fe alloy," *Applied Mechanics and Materials*, vol. 365-366, pp. 1003–1006, 2013.
- [16] C. Ran, Z. Sheng, P. Chen, W. Zhang, and Q. Chen, "Effect of microstructure on the mechanical properties of Ti-5Al-5Mo-5V-1Cr-1Fe alloy," *Materials Science and Engineering: A*, vol. 773, Article ID 138728, 2020.

- [17] B. Jiang, S. Emura, and K. Tsuchiya, "Improvement of ductility in Ti-5Al-5Mo-5V-3Cr alloy by network-like precipitation of blocky α phase," *Materials Science and Engineering: A*, vol. 722, no. apr. 11, pp. 129–135, 2018.
- [18] X.-a. Nie, Z. Hu, H.-q. Liu et al., "High temperature deformation and creep behavior of Ti-5Al-5Mo-5V-1Fe-1Cr alloy," *Materials Science and Engineering: A*, vol. 613, no. 9, pp. 306–316, 2014.
- [19] O. M. Ivasyshyn, P. E. Markov's'kyi, and I. M. Havrysh, "formation of the microstructure and mechanical properties of VT22 titanium alloy under nonequilibrium conditions of rapid heat treatment," *Materials Science*, vol. 51, no. 2, pp. 158–164, 2015.
- [20] O. M. Ivasishin, P. E. Markovsky, Y. V. Matviychuk, S. L. Semiatin, C. H. Ward, and S. Fox, "A comparative study of the mechanical properties of high-strength β -titanium alloys," *Journal of Alloys and Compounds*, vol. 457, no. 1-2, pp. 296–309, 2008.
- [21] O. M. Ivasishin, P. E. Markovsky, S. L. Semiatin, and C. H. Ward, "Aging response of coarse- and fine-grained β titanium alloys," *Materials Science & Engineering A*, vol. 405, no. 1/2, pp. 296–305, 2005.
- [22] O. M. Ivasishin, P. E. Markovsky, Y. V. Matviychuk, and S. L. Semiatin, "Precipitation and recrystallization behavior of beta titanium alloys during continuous heat treatment," *Metallurgical and Materials Transactions A*, vol. 34, no. 1, pp. 147–158, 2003.
- [23] Y.-Q. Jiang, Y. C. Lin, X.-Y. Zhang, C. Chen, Q.-W. Wang, and G.-D. Pang, "Isothermal tensile deformation behaviors and fracture mechanism of Ti-5Al-5Mo-5V-1Cr-1Fe alloy in β phase field," *Vacuum*, vol. 156, pp. 187–197, 2018.
- [24] S. Nag, Y. Zheng, R. E. A. Williams et al., "Non-classical homogeneous precipitation mediated by compositional fluctuations in titanium alloys," *Acta Materialia*, vol. 60, no. 18, pp. 6247–6256, 2012.
- [25] Y. M. Zhu, S. M. Zhu, M. S. Dargusch, and J. F. Nie, "HAADF-STEM study of phase separation and the subsequent α phase precipitation in a β -Ti alloy," *Scripta Materialia*, vol. 112, pp. 46–49, 2016.
- [26] S. Antonov, R. Shi, D. Li et al., "Nucleation and growth of α phase in a metastable β -Titanium Ti-5Al-5Mo-5V-3Cr alloy: influence from the nano-scale, ordered-orthorhombic O" phase and α compositional evolution," *Scripta Materialia*, vol. 194, Article ID 113672, 2021.
- [27] R. Dong, H. Kou, Y. Zhao, X. Zhang, L. Yang, and H. Hou, "Morphology characteristics of α precipitates related to the crystal defects and the strain accommodation of variant selection in a metastable β titanium alloy," *Journal of Materials Science & Technology*, vol. 95, pp. 1–9, 2021.
- [28] Y. C. Lina, Li-H. Wang, Q. Wu, Yi-W. Xiao, H. Cheng, and X.-Y. Zhang, "Effects of solution temperature and cooling rate on α phases and mechanical properties of a forged Ti-55511 alloy," *Materials Research Express*, vol. 6, no. 11, pp. 0–22, 2019.
- [29] O. M. Ivasishin and G. Lütjering, "Structure and mechanical properties of high-temperature titanium alloys after rapid heat treatment," *Materials Science and Engineering: A*, vol. 168, no. 1, pp. 23–28, 1993.
- [30] O. M. Ivasishin, P. E. Markovskii, and S. P. Oshkaderov, "Investigation of rapid heating of titanium alloys for hardening," *Metal Science and Heat Treatment*, vol. 32, no. 1, pp. 32–35, 1990.
- [31] O. M. Ivasyshyn, P. E. Markov's'kyi, I. M. Havrysh, and O. P. Karasev's'ka, "Influence of cooling rate in the process of hardening on the aging and formation of the mechanical characteristics of VT22 titanium alloy," *Materials Science*, vol. 50, no. 1, pp. 62–69, 2014.
- [32] P. E. Markovsky, V. I. Bondarchuk, and O. M. Herasymchuk, "Influence of grain size, aging conditions and tension rate on the mechanical behavior of titanium low-cost metastable beta-alloy in thermally hardened condition," *Materials Science & Engineering A*, vol. 645, Article ID 150162, 2015.
- [33] Z. Lei, Y. Chen, S. Ma, H. Zhou, J. Liu, and X. Wang, "Influence of aging heat treatment on microstructure and tensile properties of laser oscillating welded TB8 titanium alloy joints," *Materials Science and Engineering: A*, vol. 797, Article ID 140083, 2020.
- [34] M. Ahmed, D. G. Savvakina, O. M. Ivasishin, and E. V. Pereloma, "The effect of ageing on microstructure and mechanical properties of powder Ti-5Al-5Mo-5V-1Cr-1Fe alloy," *Materials Science and Engineering: A*, vol. 605, pp. 89–97, 2014.
- [35] Q. Lai, L. Brassart, O. Bouaziz et al., "Influence of martensite volume fraction and hardness on the plastic behavior of dual-phase steels: experiments and micromechanical modeling," *International Journal of Plasticity*, vol. 80, pp. 187–203, 2016.
- [36] C. Ran, P. Chen, L. Li, W. Zhang, Y. Liu, and X. Zhang, "High-strain-rate plastic deformation and fracture behaviour of Ti-5Al-5Mo-5V-1Cr-1Fe titanium alloy at room temperature," *Mechanics of Materials*, vol. 163, no. jan. pp. 3–10, 2017.